

## **Electronic Supplementary Information (ESI)**

Ferromagnetic coupling and spin canting behaviour in heterobimetallic  $\text{Re}^{\text{IV}}\text{M}^{\text{II}/\text{III}}$  ( $\text{M} = \text{Co}^{\text{II}/\text{III}}, \text{Ni}^{\text{II}}$ ) species

**José Martínez-Lillo,<sup>\*a,b</sup> Donatella Armentano,<sup>\*b</sup> Giovanni De Munno,<sup>b</sup> Miguel Julve,<sup>a</sup> Francesc Lloret<sup>a</sup> and Juan Faus<sup>a</sup>**

*a)* Departament de Química Inorgànica/Instituto de Ciencia Molecular, Facultat de Química de la Universitat de València, Dr. Moliner 50, 46100, Burjassot, Valencia, Spain. E-mail: [lillo@uv.es](mailto:lillo@uv.es)

*b)* Centro di Eccellenza CEMIF.CAL, Dipartimento di Chimica, Università degli Studi della Calabria, via P. Bucci 14/c, 87030 Arcavacata di Rende, Cosenza, Italy. E-mail: [donatella.armentano@unical.it](mailto:donatella.armentano@unical.it).

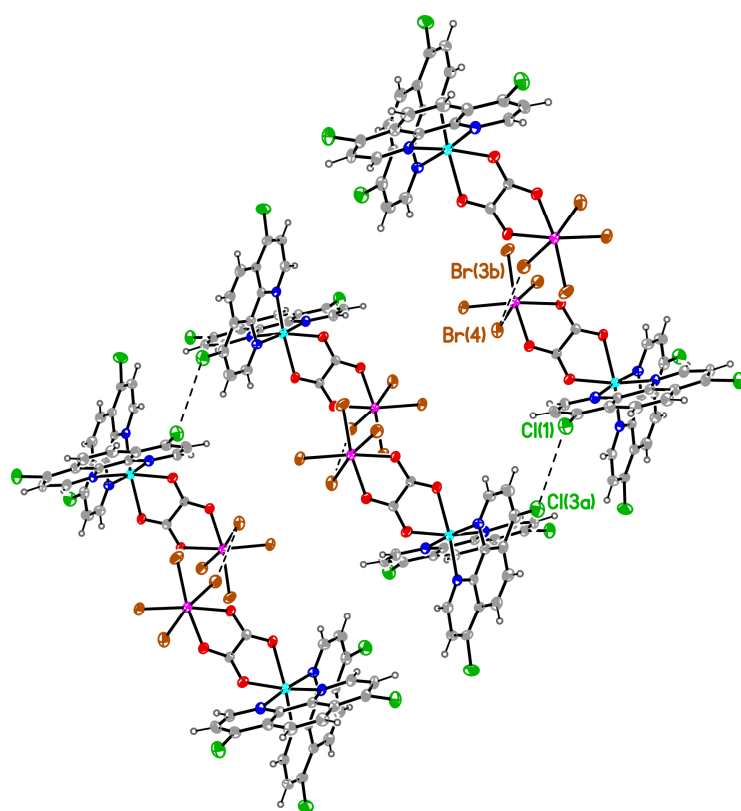


**Figure S1.** View of the shortest  $\text{Cl}\cdots\text{Cl}$  and  $\text{Br}\cdots\text{Br}$  intermolecular distances in **1** [3.685(1) and 5.623(1) Å, respectively].

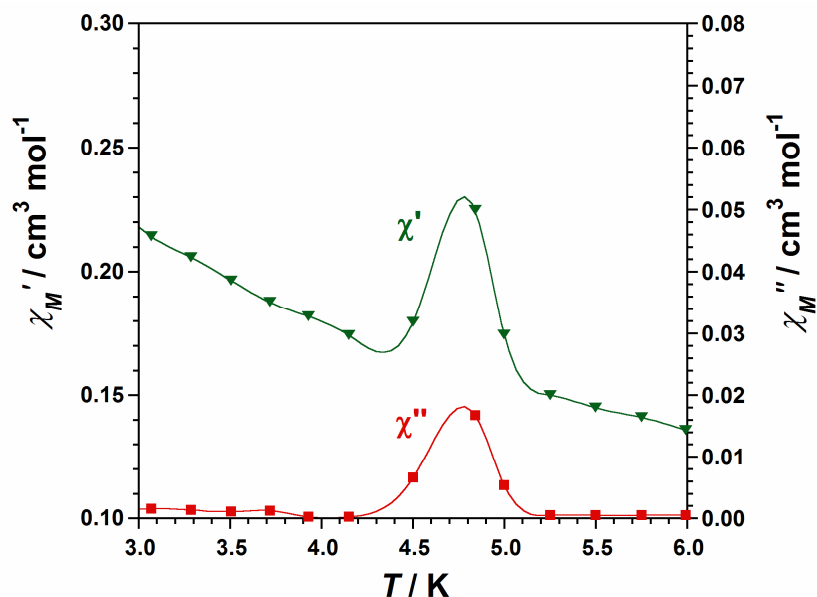


**Figure S2.** Thermal dependence of the in-phase ( $\chi_M'$ ) and out-of-phase ( $\chi_M''$ ) ac susceptibility signals for **3** under an oscillating magnetic field of  $\pm 1$  G and a frequency of 330 Hz.

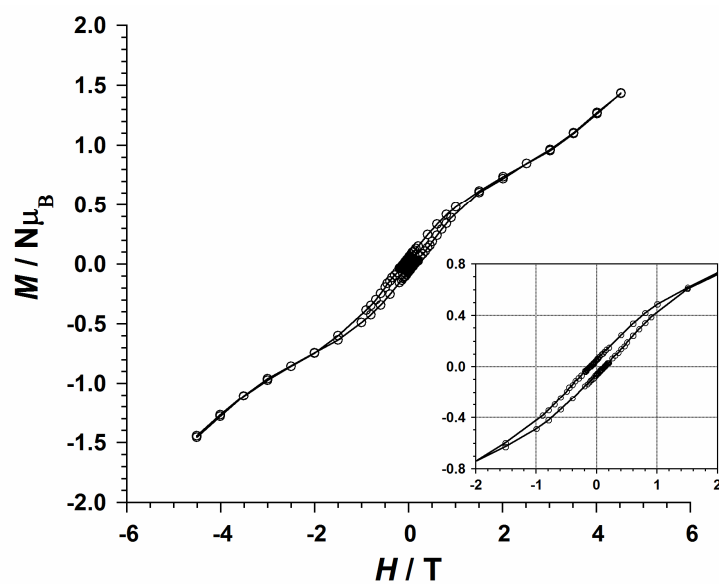


**Figure S3.** Variable-field magnetization data for **3** at 2.0 K. The solid line is an eye guide. The inset shows a detail of the hysteresis loop.

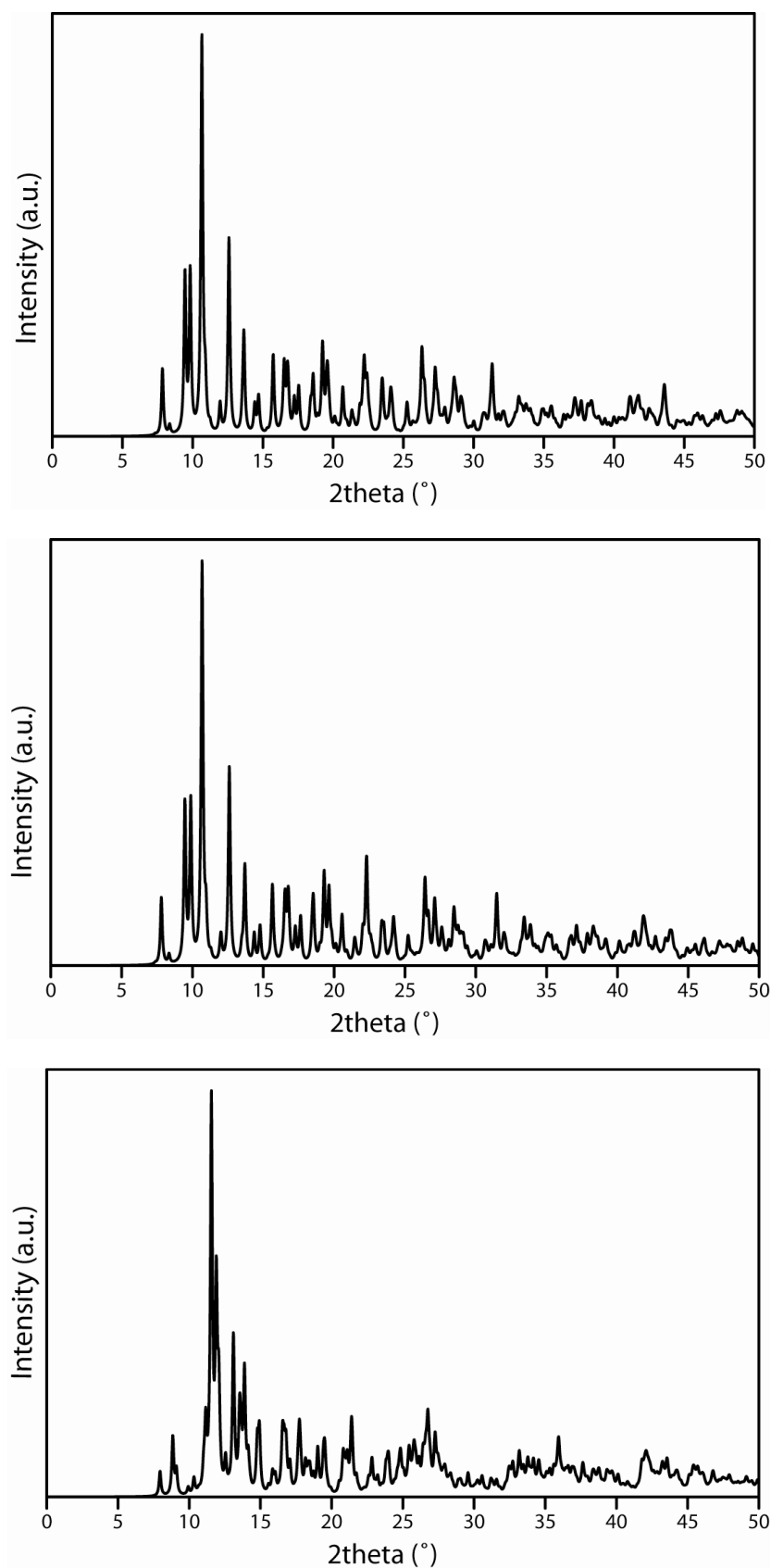


**Figure S4.** PXRD plots for samples of compounds **1** (top), **2** (middle) and **3** (bottom).